THERMOPHYSICAL PARAMETERS AND ENTHALPY-TEMPERATURE CURVE OF PHASE CHANGE MATERIAL WITH SUPERCOOLING FROM T-HISTORY DATA

Inge Magdalena SUTJAHJA[1], Alfriska SILALAHI[2], Daniel KURNIA[3], Surjamanto WONORAHARDJO[4]

The thermophysical parameters of a phase change material (PCM) are important for the determination of its performance in thermal energy storage (TES). These parameters include the solid and liquid specific heats ($c_{p,s}$ and $c_{p,l}$, respectively) and the specific heat of fusion, which is related to the solid–liquid phase change. In addition to the constant values of these parameters, for materials that do not have a clearly-defined phase transition, the enthalpy-temperature curve $h(T)$ is very useful. An analysis of $h(T)$ revealed the effective thermal capacity as a function of the temperature $c_{p,\text{eff}}(T)$. Its constant values at the low and high temperature regions correspond to the $c_{p,s}$ and $c_{p,l}$ values, respectively. In this study, the thermophysical parameters and $h(T)$ curve of an inorganic PCM $CaCl_2{\cdot}6H_2O$ are investigated using a T-history data analysis. The data analysis is performed according to the method reported by Zhang, and its subsequent modification by Hong, while the $h(T)$ curve is obtained by adopting the method proposed by Marín. The $h(T)$ curve is fitted using a recent mathematical model for the solidification process including supercooling.

Keywords: thermophysical parameters; specific enthalpy-temperature curve; T-history; phase change material; $CaCl_2{\cdot}6H_2O$; erf function.

1. Introduction

Phase change materials (PCM) can be employed in thermal energy storage (TES) and are one of the promising materials for an energy conservation. Compared with a sensible TES, they can store a relatively large quantity of

[1] Magnetic and Photonics Research Group, Institut Teknologi Bandung, Indonesia, e-mail: ingesansansan@gmail.com,
[2] Magnetic and Photonics Research Group, Institut Teknologi Bandung, Indonesia, e-mail: alfriska.silalahi@gmail.com
[3] Magnetic and Photonics Research Group, Institut Teknologi Bandung, Indonesia, e-mail: daniel@fi.itb.ac.id
[4] Building Technology, Institut Teknologi Bandung, Indonesia, e-mail: surjamanto.wonorahardjo@gmail.com

thermal energy at a relatively constant temperature around its phase change (solid–liquid) transition region [1–4]. A PCM can work periodically, as the stored heat is released back to the environment when the ambient air temperature is lower than the temperature of the material. The most important thermophysical parameters of a PCM are the solid and liquid specific heats ($c_{p,s}$ and $c_{p,l}$) and specific heat of fusion (Δh) that is related to the solid–liquid phase transition. In addition to these constant parameters, for a real material that does not have a clearly-defined phase transition, such as a material that experiences a non-isothermal phase change, the specific enthalpy-temperature $h(T)$ curve should be considered; $h(T)$ determines the density of the heat storage capacity according to the equation [5]:

$$q = \int_{T_{ref}}^{T} c_p(T)dT + h_0 = h(T) \tag{1}$$

where q is the heat per unit mass, $c_p(T)$ is the thermal capacity function, and $h_0 = h(T_{ref})$ is the value of the enthalpy at the reference temperature T_{ref} . Figure 1 shows the schematic of the specific enthalpy curve of an ideal and real PCM.

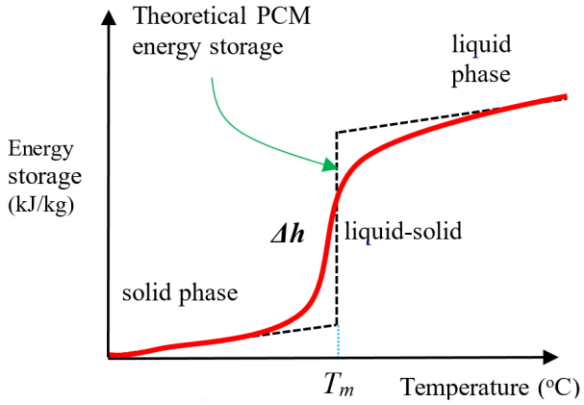

Fig. 1. Schematic of the specific enthalpy curve of an ideal (black dashed line) and real PCM (red solid line).

The T-history method, introduced for the first time by Zhang [6], is a simple method to characterise the thermophysical properties of PCMs. Compared with common methods such as the differential scanning calorimetry (DSC), the data obtained using the T-history method is more reliable and represents the general intrinsic properties of the studied material, as it analyses a relatively large amount of the sample (~ 10 g, compared with ~ 10 mg of sample for a DSC measurement) [7]. In the initial data analysis method reported by Zhang, the

concept of energy balance between the PCM and water as a reference material in certain phase boundaries have revealed a set of thermophysical parameters of the PCM including the constants $c_{p,s}$, $c_{p,l}$, and Δh. This method has been improved by Hong et al. [8] to include the liquid and solid sensible contributions in the phase change region, including the end of the phase change boundary, using the inflection point of the derivative of the temperature with respect to the measurement time.

In order to obtain the enthalpy-temperature curve, an analysis of T-history data has been proposed by Marín et al. [9], Sandnes and Rekstad [10], and Kravvaritis et al. [11]; a review has been reported by Solé et al. [12]. The extensive studies performed by D'Avignon and Kummert [13] showed that the method proposed by Marín et al. [9] is the most appropriate to reveal the enthalpy-temperature curve of PCMs, in particular, for a (heterogeneous) salt hydrate. In these studies, the T-history measurements were, in general, performed during the solidification, where a supercooling effect commonly emerges for an inorganic PCM. However, the occurrence of a supercooling has not been properly treated in the enthalpy curve, in particular, for the determination of the enthalpy jump, Δh. The Δh value is related to the difference of the enthalpy between a well-ordered crystalline solid that has a low entropy and significantly-less-ordered liquid phase that has a high entropy.

In this study, we determine the thermophysical parameters of the inorganic PCM $CaCl_2 \cdot 6H_2O$ that experience a significant supercooling, by comparing the results of two different data analyses, i.e., using the constant values of the parameters and enthalpy-temperature curve. We review the T-history method and its mathematical model for a data analysis, reported in the studies performed by Zhang et al. [6], Hong et al. [8], and Marín et al. [9]. The enthalpy-temperature curve is then fitted using a recent mathematical model for the solidification process including a supercooling, developed by Uzan et al. [14]. This model assumes that the phase change process occurs within a specific temperature range, hence $c_p(T)$ can be expressed as a Gaussian pulse. By expressing the enthalpy function $h(T)$ as an integral of $c_p(T)$ (Eq. 1), they obtained that the enthalpy function can be expressed by the error function (*erf*).

2. Review of the T-history analysis

2.1 Constant specific enthalpy of the PCM

In the initial report by Zhang [6] and its modification by Hong [8], the analysis of the T-history data for the PCM and water started by determining the phase boundaries that signify the release of sensible and latent heats during the cooling process. Figure 2 illustrates the cooling process of the PCM and water as a reference material; the phase boundaries of the PCM and water that include the

phase region, temperature range, time period, and area for further analysis of the T-history data, are outlined in Table 1.

Upon cooling from T_0, with T_0 is higher than the melting or solidification temperature T_m, the molten PCM experiences a temperature change and liquid-to-solid phase transition. The supercooling temperature is denoted by T_s, while the difference between T_s and T_m is referred to as a supercooling degree $(\Delta T_m = T_m - T_s)$.

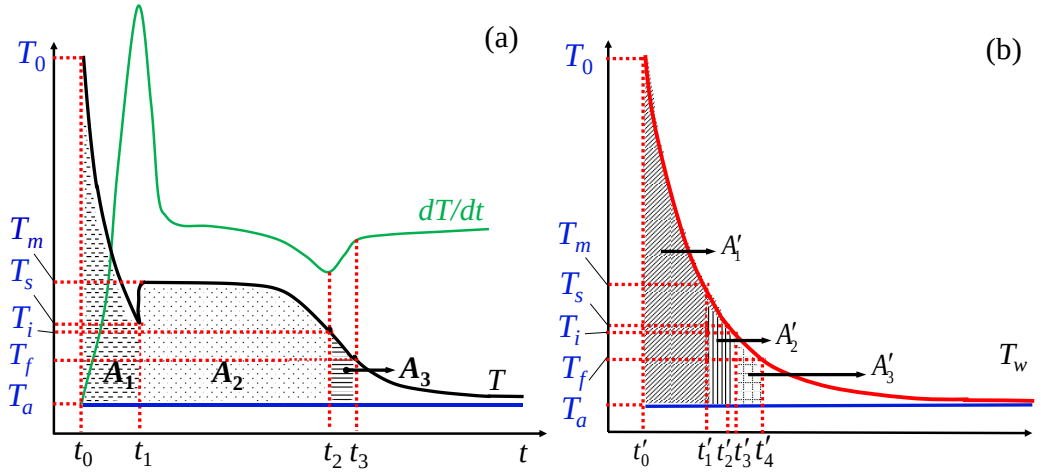

Fig. 2. Schematic of T-history data for cooling of: (a) PCM including a supercooling, shown along with its derivative curve and (b) water as a reference. The phase boundaries and area below the temperature graph for the determination of the thermophysical parameters are shown in Table 1.

Table 1

Phase region, temperature range, time period, and areas of each T-history curve of the PCM and water as a reference material for a further data analysis.

Material	Phase region	Temperature Range	Time period	Area
PCM	Sensible liquid	$T_0 - T_s$	$t_0 - t_1$	A_1
	Phase change	$T_s - T_m - T_i$	$t_1 - t_2$	$+A_2$
	Sensible solid	$T_i - T_f$	$t_2 - t_3$	A_3
Reference material	Sensible liquid	$T_0 - T_s$	$t'_0 - t'_2$	A'_1
	Sensible liquid	$T_m - T_i$	$t'_1 - t'_3$	A'_2
	Sensible liquid	$T_i - T_f$	$t'_3 - t'_4$	A'_3

The heat release of a PCM consist of a sensible and latent heats. The temperature remains constant during the latent heat release at the phase transition at a value of T_m, and it exponentially decreases during the cooling process that

accompanies the sensible heat. On the other hand, the heat release of the water in this temperature region consist only of the sensible heat, which signifies the monotonous decrease of the temperature with the time. Using the procedure introduced by Hong et al. [8], the end of the phase transition process was determined from the inflection point of the first time derivative of the T-history curve (Fig. 2(a)), denoted by T_i. In addition, t_3 and its corresponding T_f represent the transformation of the overall PCM when it becomes a solid. The energy equations for the PCM and water are shown in Table 2.

Table 2

The energy equations for the PCM and water as a reference material.

Phase region	PCM	Area
liquid	$\left(m_{t,p}\cdot c_{p,t}+m_p\cdot c_{p,l}\right)\left(T_0-T_s\right)=\alpha\cdot A_c\cdot A_1$	$A_1=\int_{t_0}^{t_1}\left(T-T_a\right)dt$
liquid–solid	$\left(m_{t,p}\cdot c_{p,t}+m_p\cdot\frac{c_{p,l}+c_{p,s}}{2}\right)\left(T_m-T_i\right)+m_p\cdot\Delta h=\alpha\cdot A_c\cdot A_2$	$A_2=\int_{t_1}^{t_2}\left(T-T_a\right)dt$
Solid	$\left(m_{t,p}\cdot c_{p,t}+m_p\cdot c_{p,s}\right)\left(T_i-T_f\right)=\alpha\cdot A_c\cdot A_3$	$A_3=\int_{t_2}^{t_3}\left(T-T_a\right)dt$
	Reference material (water)	
liquid	$\left(m_{t,w}\cdot c_{p,t}+m_w\cdot c_{p,w}\right)\left(T_0-T_s\right)=\alpha\cdot A_c\cdot A_1'$	$A_1'=\int_{t_0'}^{t_2'}\left(T'-T_a\right)dt$
liquid	$\left(m_{t,w}\cdot c_{p,t}+m_w\cdot c_{p,w}\right)\left(T_m-T_i\right)=\alpha\cdot A_c\cdot A_2'$	$A_2'=\int_{t_1'}^{t_3'}\left(T'-T_a\right)dt$
liquid	$\left(m_{t,w}\cdot c_{p,t}+m_w\cdot c_{p,w}\right)\left(T_i-T_f\right)=\alpha\cdot A_c\cdot A_3'$	$A_3'=\int_{t_3'}^{t_4'}\left(T'-T_a\right)dt$

In the above equations, α is the heat transfer coefficient between the tube and air environment, A_c is the convective heat-transfer area of the tube, m_p and m_w, and $m_{t,p}$ and $m_{t,w}$ are the masses of the PCM and water, and those of the tubes used for the PCM and water, respectively, $c_{p,w}$ is the specific heat of water, $c_{p,t}$ is the specific heat of the tube material, $c_{p,l}$ and $c_{p,s}$ are the specific heats of a liquid and solid PCM, and Δh is the specific heat of fusion of the PCM. The values of

$\{A_1, A_2, A_3\}$ and $\{A_1', A_2', A_3'\}$ correspond to the areas below the curves of the PCM and water temperatures with respect to that of the air environment, respectively; they correspond to the boundaries shown in Table 1.

The thermophysical parameters of the PCM can be obtained using the above method [8]:

$$c_{p,l} = \left(\frac{m_{t,w} \cdot c_{p,t} + m_w \cdot c_{p,w}}{m_p} \cdot \frac{A_1}{A_1'} \right) - \frac{m_{t,p}}{m_p} \cdot c_{p,t} \tag{2}$$

$$c_{p,s} = \left(\frac{m_{t,w} \cdot c_{p,t} + m_w \cdot c_{p,w}}{m_p} \cdot \frac{A_3}{A_3'} \right) - \frac{m_{t,p}}{m_p} \cdot c_{p,t} \tag{3}$$

$$\Delta h = \left(\frac{m_{t,w} \cdot c_{p,t} + m_w \cdot c_{p,w}}{m_p} \cdot \frac{A_2}{A_2'} \cdot (T_m - T_i) \right) - \left(\frac{m_{t,p}}{m_p} \cdot c_{p,t} + \frac{c_{p,l} + c_{p,s}}{2} \right) \cdot (T_m - T_i) \tag{4}$$

2.2 Specific enthalpy-temperature curve of the PCM

Marín [9] introduced the concept of enthalpy and its relationship with temperature by evaluating the energy absorption/release of a PCM in a small interval $\Delta T_j = T_{j+1} - T_j$ that corresponds to the time interval $\Delta t_j = t_{j+1} - t_j$:

$$m_p \cdot \Delta h(T_j) + m_t \cdot c_{p,t} \cdot (T_j - T_{j+1}) = \alpha \cdot A_c \cdot A_j \tag{5}$$

where $\Delta h(T_j)$ is the specific enthalpy change of the PCM in the interval ΔT_j (T_j is the average temperature in this interval), and $A_j = \int_{t_j}^{t_j + \Delta t_j} (T - T_a) dt$ is the corresponding area for the PCM. A similar equation is obtained for water as a reference material in a small interval $\Delta T_j' = T_{j+1}' - T_j'$ that corresponds to the time interval $\Delta t_j' = t_{j+1}' - t_j'$:

$$(m_t \cdot c_{p,t} + m_w \cdot c_{p,w})(T_j' - T_{j+1}') = \alpha \cdot A_c \cdot A_j' \tag{6}$$

where $A_j' = \int_{t_j'}^{t_j' + \Delta t_j'} (T' - T_a) dt$ is the corresponding area for water. By dividing Eqs. (5) and (6), it is obtained that $\Delta h(T_j)$ is:

$$\Delta h(T_j) = \left(\frac{m_t \cdot c_{p,t} + m_w \cdot c_{p,w}}{m_p} \right) \cdot \frac{A_j}{A_j'} \cdot \Delta T_j' + \frac{m_t}{m_p} \cdot c_{p,t} \cdot \Delta T_j \tag{7}$$

The specific enthalpy-temperature curve $h(T)$ can be obtained by summing $\Delta h(T_j)$ over the whole temperature region, and adding to this sum a constant value h_0, so that the enthalpy at a low temperature is equal to zero:

$$h(T) = \sum_{i=1}^{N} \Delta h(T_j) + h_0 \tag{8}$$

3. Methods

For this study, we used the salt hydrate $CaCl_2 \cdot 6H_2O$, purchased from Sigma Aldrich. For the measurements, we used a test tube that has a length of approximately 250 mm, an inner diameter of approximately 10 mm, and a glass thickness of approximately 1 mm. The dimensions of the test tube were chosen so that they satisfy the condition that the Biot number $(\mathrm{Bi} = \alpha R/2\kappa)$ is smaller than 0.1, in order to employ the lumped capacitance method [15]; α is the natural convective heat-transfer coefficient between the tube and air environment, R is the radius of the tube, and κ is the thermal conductivity of the PCM.

Two different tubes that contain a molten $CaCl_2 \cdot 6H_2O$ and water as a reference material are equipped with a temperature sensor that is located in the centre along the tube axis. In another setup, two thermocouples are placed at several positions along the tubes, i.e.: (i) at the centre along the tube axis, and (ii) at the inner circumference of the tube, parallel to the first sensor. This enables to evaluate the homogeneity of the temperature and phase change process along the radial direction. The sensors are T-type thermocouples that have a diameter of approximately 1 mm and were connected to a data logger (Applent AT4508A, Instrument Inc.).

Prior to the measurement, the tubes are heated to reach the same temperature, which is above the melting temperature of $CaCl_2 \cdot 6H_2O$ ($T_m \sim 29$ °C). The tubes are then placed in a cool air environment provided by the adiabatic controlled chamber. Then, their temperature history upon cooling is measured using the temperature sensors and recorded using the data logger connected to a PC computer. The measurement is repeated three times to ensure data repeatability.

4. Results and Discussion

The T-history graphs of the temperature as a function of time of $CaCl_2 \cdot 6H_2O$, using water as a reference material are shown in Fig. 3, where the sensor is at the centre; the inset shows the radial distribution of the sample's temperature. This figure shows that starting from T_0, the temperature of the water decreases monotonously with the time. On the other hand, the temperature of

$CaCl_2 \cdot 6H_2O$ rapidly decreases with the time, and reaches the minimum value denoted as a supercooling temperature (T_s) that is significantly smaller that the melting or crystallisation temperature (T_m). The supercooling is related to the hampered latent heat release caused by the barrier that has to be overcome in the crystallisation process [16]. With a further increase of the time, the sample's temperature increases owing to the accumulation of latent heat release, before it becomes constant for a certain period of time. The sample's temperature then gradually decreases with time until it reaches the thermal equilibrium with the water and environment. Using three sets of data measurements, we obtain that the average T_m and T_s of $CaCl_2 \cdot 6H_2O$ are 28.5 °C and 20 °C, respectively; the supercooling degree is 9 °C. The value of T_m is in agreement with those obtained using DSC measurements, both in the endothermic (29.0-29.8 °C [17]) or exothermic modes [18-19]. In addition, the supercooling degree is influenced by the volume quantity, cooling rate, surface roughness, and nucleation agent mass [14].

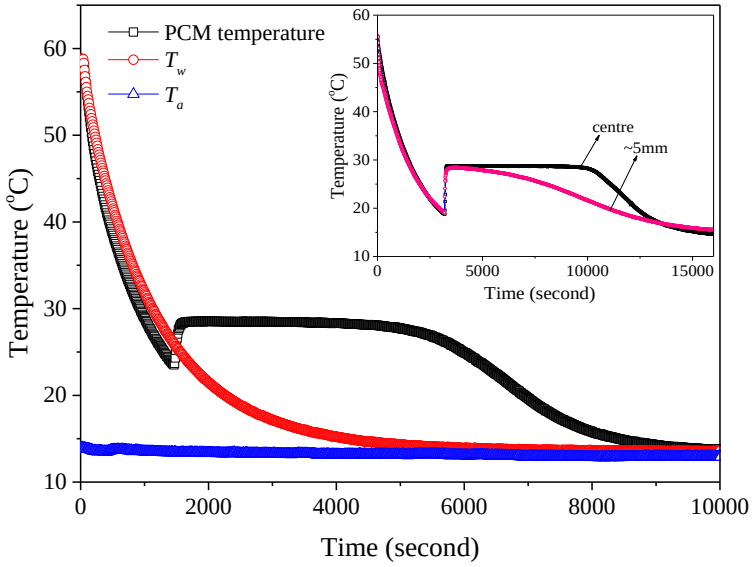

Fig. 3. Typical T-history curves of $CaCl_2 \cdot 6H_2O$ and water in a cold air environment, where the sensor is at the centre along the tube axis. The inset shows the temperature variations as a function of the sensor position: (i) at the centre and (ii) at the inner circumference of the tube and parallel to the first sensor.

The inset of Fig. 3 shows the similarity between the profiles of the temperature decrease and subcooling recorded by the sensors located at the centre and inner circumference of the tube. Therefore, the temperature distribution along the radial direction of the tube can be considered to be homogeneous. It satisfies

the assumption of one-dimensional heat transfer for a cylindrical geometry according to the lumped capacitance method. With a further increase of the time, the temperature distribution becomes non-uniform. It can be seen that the temperature values at the inner circumference rapidly decrease, as it is closer to the environment. The obtained temperature distribution is in a good agreement with that reported by Hong et al. [8]. For a further data analysis, we used the temperature data at the centre of the tube in order to obtain reliable and accurate values of the thermophysical parameters.

Prior to the data analysis, in Fig. 4 we show the temperature data $(T-t)$ and its derivative temperature curve $(dT/dt-t)$ for one set of data for $CaCl_2 \cdot 6H_2O$. In addition to the above temperature parameters, in the figure we show the kink temperature T_k, inflection temperature T_i, and final temperature T_f. The kink temperature T_k is determined as the intersection between the two linear lines in the temperature derivative curve of $CaCl_2 \cdot 6H_2O$, while T_f is determined as the deviation from the value of zero in the temperature derivative curve of $CaCl_2 \cdot 6H_2O$ (Fig. 4).

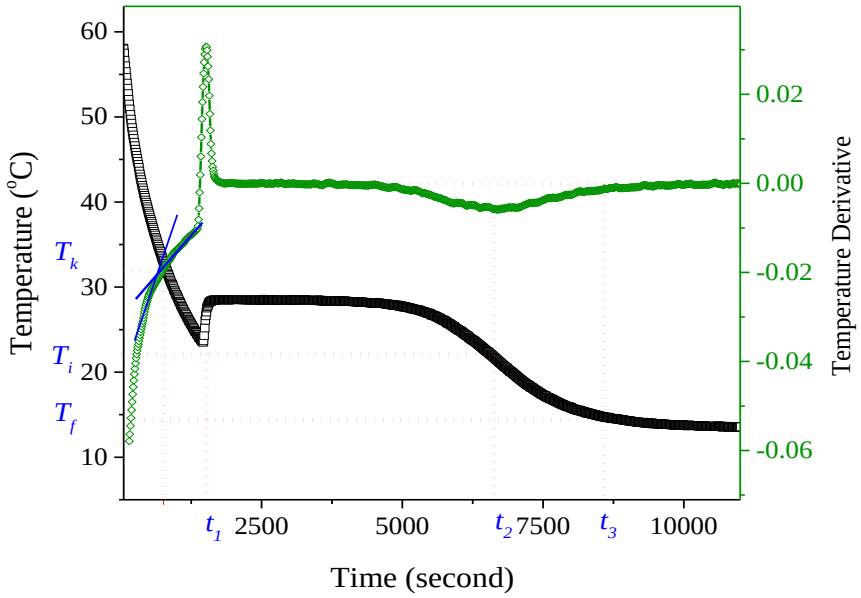

Fig. 4. T-history data of $CaCl_2 \cdot 6H_2O$ and its derivative curve. The phase transition region is limited by T_k and T_i, each of them was determined using the temperature derivative curve.

In order to analyse the data using the original method proposed by Zhang and Hong, we employ Eqs. (2), (3), and (4) to obtain the thermophysical parameters of

$CaCl_2 \cdot 6H_2O$. The obtained values of the liquid and solid specific heats ($c_{p,l}$ and $c_{p,s}$) and specific heat of fusion (Δh) using three sets of data measurements are shown in Table 3, along with the average and standard deviation values.

Table 3

The values of solid and liquid specific heats and specific enthalpy jump (specific heat of fusion) of $CaCl_2 \cdot 6H_2O$, obtained by analysing the T-history data, using the methods proposed by Zhang and Hong, and Marin.

No. of measurement	Zhang and Hong's method			Marin's method		
	$c_{p,l}$ [kJ/kg.K]	$c_{p,s}$ [kJ/kg.K]	Δh [kJ/kg]	$c_{p,l}$ [kJ/kg.K]	$c_{p,s}$ [kJ/kg.K]	Δh [kJ/kg]
1	2.18	2.30	187	3.45	2.10	195
2	2.31	2.10	181	3.48	2.21	190
3	2.15	2.07	187	3.24	2.17	196
Average values	2.21	2.16	185	3.39	2.16	194
Standard deviation	0.09	0.13	3	0.07	0.06	3

The specific enthalpy-temperature curve obtained by analysing the T-history data using Marín's method (Eq. 8) is shown in Fig. 5, along with the material's phase state for each phase region. Using a magnified view of the DSC curve of $CaCl_2.6H_2O$ shown in Ref. [18–20], we found that the positions of inflection point T_i and kink T_k resemble the low- and high-temperatures of the peaks of the DSC curve, respectively, and therefore they can be related to the beginning and end of the latent heat period in the T-history measurement. In other words, the phase transition region is limited by T_k and T_i, and the region between T_s and T_m corresponds to the (metastable) supercooled liquid before the nucleation process at T_s [16]. The difference of enthalpy values between T_k and T_i reveals the value of Δh, and it determines the unique combination of pressure and temperature at which the substance can exist in either, or both, phase states, depending on the system's total heat content or enthalpy [16].

Using the results reported in Ref. [14], the enthalpy curve of $CaCl_2 \cdot 6H_2O$ around its phase change region can be fitted by the error function (*erf*):

$$h(T) = c_p(T - T_m) + \frac{\Delta h}{2} erf\left(\frac{T - T_m}{\delta T}\right) \tag{9}$$

where δT is half of the temperature range of the phase change. The fitting enthalpy curve of $CaCl_2 \cdot 6H_2O$ is represented with the blue line in Fig. 5. One can see that this error function is fairly good to describe the phase transition behaviour of $CaCl_2 \cdot 6H_2O$ from T_i to T_k.

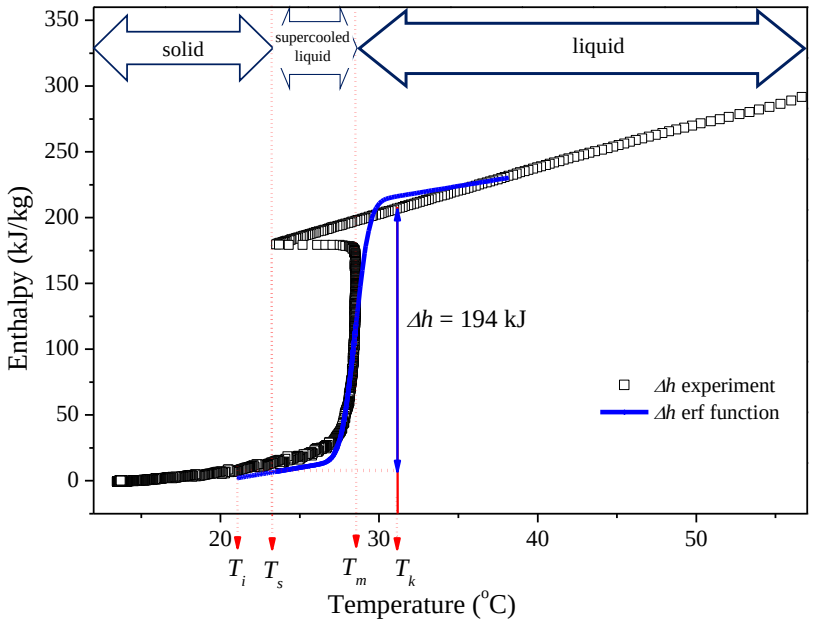

Fig. 5. Enthalpy-temperature curve of $CaCl_2 \cdot 6H_2O$ obtained using Marin's method; it contains the solid, supercooled liquid, and liquid phases. The solid blue line represent the fitting enthalpy curve using error function, while the dashed red line represents the linear fit at high temperatures.

Using the $h(T)$ curve, the effective thermal capacity function $c_{p,\text{eff}}(T)$ can be easily determined by a differentiation [11, 21]:

$$c_{p,\text{eff}} = \frac{\partial h(T)}{\partial T} \tag{10}$$

The experimentally determined $c_{p,\text{eff}}(T)$ of $CaCl_2 \cdot 6H_2O$ is shown in Fig. 6. It shows that $c_{p,\text{eff}}$ has two constant values at the low and high temperature phases related to the solid and liquid specific heats, respectively; it has a peak in-between these regions at a temperature of approximately 28.5 °C, owing to the enthalpy jump. In order to check the accuracy of the obtained values, one might determine $c_{p,s}$ at $T \le T_i$ and $c_{p,l}$ at $T \ge T_k$. The average values of Δh, $c_{p,s}$, and $c_{p,l}$ of $CaCl_2 \cdot 6H_2O$ obtained using Marín's method based on the $h(T)$ curve, are shown in Table 3. It can be seen that both models (Zhang/Hong and Marín) show that $c_{p,s}$ is smaller than $c_{p,l}$; the $c_{p,l}$ value obtained using Marín's method is larger than that obtained by the Zhang/Hong method. In addition, the average value of the specific enthalpy jump is in a good agreement with the specific heat of fusion.

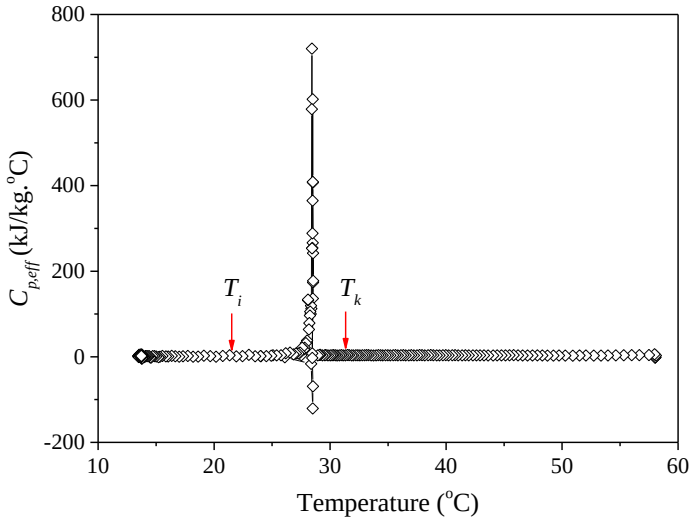

Fig. 6. Effective thermal capacity of $CaCl_2 \cdot 6H_2O$ as a function of the temperature.

For further analysis, Table 4 shows a comparison of the corresponding values reported in the literature, obtained by the same T-history method with various data analyses or by a DSC.

Table 4

Comparison between the thermophysical parameters of $CaCl_2 \cdot 6H_2O$ obtained in this study and those reported in other studies based on the same T-history method (THM) and DSC.

Experimental method	Measurement/ analysis method	$c_{p,l}$ [kJ/kg·K]	$c_{p,s}$ [kJ/kg·K]	Δh [kJ/kg]	Reference
THM	Zhang/Hong	2.21	2.16	185	This study
THM	Marin	3.39	2.16	194	This study
THM	Zhang	2.2	1.77	210	[18]
DSC	Exothermic	1.9	1.6	212	[18]
DSC	Exothermic	2.1	1.4	140	[19]
DSC	Endothermic			190.8	[22]
DSC	Endothermic			160	[20]

In addition to the Δh values shown in the table, a recent review paper [17] reported the same wide range of values obtained using a DSC. It was recommended that the value of 198 kJ/kg is the most appropriate for the heat of fusion of $CaCl_2 \cdot 6H_2O$ based on a high precision adiabatic calorimeter measurement. It was obtained that there is a good agreement between the thermophysical parameters values of $CaCl_2 \cdot 6H_2O$ obtained using the T-history

data and DSC. This confirms the validity of the T-history analysis method. The agreement between the parameters values obtained using the Zhang and Hong', and Marín's methods is likely to be guaranteed when the ratio between the diameter and length of the tube is larger than 15.

4. Conclusion

Thermophysical parameters and specific enthalpy–temperature curves that can be employed to reveal the performance of a PCM were obtained for inorganic PCM $CaCl_2 \cdot 6H_2O$, using the methods proposed by Zhang and Hong, and Marín. This material is a real material that provides significant supercooling during the crystallisation process following the latent heat release at a high temperature. The liquid–solid phase transition observed in the enthalpy-temperature curve is limited by the kink (T_k) and inflection (T_i) temperatures with sharp transition at solidification temperature (T_m). The region between supercooling temperature (T_s) and T_m corresponds to the (metastable) supercooling melt before the nucleation process. We revealed that the error function is appropriate to represent the behaviour of the enthalpy-temperature curve around its phase transition region. The temperature derivation of the enthalpy reveals the effective thermal capacity function, $c_{p,\text{eff}}(T)$. Its constant values at the low $(T \le T_i)$ and high $(T \ge T_k)$ temperature regions are related to the solid and liquid specific heats ($c_{p,s}$ and $c_{p,l}$), respectively. Furthermore, we compared the thermophysical parameters ($c_{p,s}$, $c_{p,l}$, and Δh) of $CaCl_2 \cdot 6H_2O$ obtained using the T-history data analysis, according to the methods proposed by Zhang and Hong, and Marín, with those reported in the literature obtained using the same methods and DSC.

Acknowledgment

This research is financially supported by the Kementrian Riset Teknologi dan Pendidikan Tinggi Indonesia through the Desentralisasi 2016 research program under the contract number: 583p/I1.C01/PL/2016.

R E F E R E N C E S

[1]. *I. Dinçer, M. A. Rosen*, "Thermal energy storage: systems and applications", 2nd Edn. John Wiley & Sons, Ltd, United Kingdom 2011.
[2]. *A. S. Fleischer*, Thermal energy storage using phase change materials. Fundamentals and applications, Springer, 2015.
[3]. *H. Mehling and L. F. Cabeza*, Heat and cold storage with PCM: An up to date introduction into basics and applications, Springer, Germany 2008.
[4]. *A. Sharma, K. K. Sanjay (Editors)*: Energy sustainability through green energy. Thermal energy storage (part IV). Springer, India 2015.

[5]. *M. J. Moran, H. N. Shapiro, D. D. Boettner, and M. B. Bailey*, Fundamentals of Engineering Thermodynamics, 8th Edn. John Wiley & Sons, Inc. 2014.
[6]. *Y. Zhang, Y. Jiang, and Y. Jiang*, "A simple method, the T-history method, of determining the heat of fusion, specific heat and thermal conductivity of phase-change materials", Meas. Sci. Technol. **10**(1999), 201–205.
[7]. *E. Günther, S. Hiebler, H. Mehling, R. Redlich*, "Enthalpy of phase change materials as a function of temperature: required accuracy and suitable measurement methods", Int. J. Thermophys. **30**(2009), 1257–1269, DOI 10.1007/s10765-009-0641-z.
[8]. *H. Hong, S. K. Kimb, Y.-S. Kim*, "Accuracy improvement of T-history method for measuring heat of fusion of various materials", Int. J. Refrigeration **27**(2004), 360–366, DOI:10.1016/j.ijrefrig.2003.12.006.
[9]. *J. M. Marín, B. Zalba, L. F. Cabeza, H. Mehling*, "Determination of enthalpy–temperature curves of phase change materials with the temperature-history method: improvement to temperature dependent properties", Meas. Sci. Technol. **14**(2003), 184–189.
[10]. *B. Sandnes, J. Rekstad*, "Supercooling salt hydrates: stored enthalpy as a function of temperature", Sol. Energy **80**(2006), 616–625.
[11]. *E. D. Kravvaritis, K. A. Antonopoulos, C. Tzivanidis*, "Improvements to the measurement of the thermal properties of phase change materials", Meas. Sci. Technol. **21**(2010), 045103, 1–9, DOI: 10.1088/0957-0233/21/4/045103.
[12]. *A. Solé, L. Miró, C. Barreneche, I. Martorell, L. F. Cabeza*, "Review of the T-history method to determine thermophysical properties of phase change materials (PCM)", Renew. Sust. Energy Rev. **26**(2013), 425–436, DOI: 10.1016/j.rser.2013.05.066.
[13]. *K. D'Avignon, M.Kummert*, "Assessment of T-history method variants to obtain enthalpy-temperature curves for PCMs with significant subcooling", J. Therm. Sci. Eng. Appl. **7**(2015), 041015, 1–9.
[14]. *A.Y. Uzan, Y. Kozak, Y. Korin, I. Harary, H. Mehling, G. Ziskind*, "A novel multi-dimensional model for solidification process with supercooling", Int. J. Heat Mass Transfer **106**(2017), 91-102.
[15]. *T. L. Bergman, A. S. Lavine, F. P. Incropera, D. P. Dewitt*, Fundamentals of heat and mass transfer, 7th Edn. John Wiley & Sons 2011.
[16]. *M.E. Glicksman*, Principles of solidification. Springer, New York 2011.
[17]. *M. Kenisarin, K. Mahkamov*, "Salt hydrates as latent heat storage materials: Thermophysical properties and costs", Sol. Energy Mater. Sol. Cells **145**(2016), 255–286, DOI: 10.1016/j.solmat.2015.10.029.
[18]. *A. Hasan, S. J. McCormack, M. J. Huang, B. Norton*, "Characterization of phase change materials for thermal control of photovoltaics using differential scanning calorimetry and temperature history method", Energy Convers. Manag. **81**(2014), 322–329, DOI: 10.1016/j.enconman.2014.02.042.
[19]. *V. V. Tyagi, D. Buddhi*, "Thermal cycle testing of calcium chloride hexahydrate as a possible PCM for latent heat storage", Sol. Energy Mater. Sol. Cells **92**(2008), 8, 891–899, DOI:10.1016/j.solmat.2008.02.021
[20]. *A. Abhat*, "Low temperature latent heat thermal energy storage: heat storage materials", Sol. Energy **10**(1983), 4, 313–332.
[21]. *E.D. Kravvaritis, K.A. Antonopoulos, C. Tzivanidis*, "Experimental determination of the effective thermal capacity function and other thermal properties for various phase change materials using the thermal delay method", Appl. Energy **88**(2011), 4459–4469.
[22]. *G. A. Lane*, "Low temperature heat storage with phase change materials", Int. J. Ambient Energy **1**(1980), 155–168.